

# Local detection of deep carrier traps in the pn-junction of silicon solar cells

T. Mchedlidze,<sup>1</sup> L. Scheffler,<sup>1</sup> J. Weber,<sup>1</sup> M. Herms,<sup>2</sup> J. Neusel,<sup>2</sup> V. Osinniy,<sup>2</sup> C. Möller,<sup>3</sup> and K. Lauer<sup>3</sup>

<sup>1</sup>Technische Universität Dresden, 01062 Dresden, Germany

<sup>2</sup>Bosch Solar Energy AG, Robert-Bosch-Str. 1, 99310 Arnstadt, Germany

<sup>3</sup>CiS Forschungsinstitut für Mikrosensorik und Photovoltaik GmbH, 99099 Erfurt, Germany

(Received 14 February 2013; accepted 3 May 2013; published online 1 July 2013)

Mesa-diodes, with fully preserved solar cell structure, were fabricated at various locations of silicon solar cell. Deep level transient spectroscopy was applied for detection of carrier traps in the mesa-diodes. The parameters of the traps suggest their relation to interstitial iron and/or iron-related complexes. The density of the traps sharply falls with the distance from the pn-junction. Measurements using Schottky-diodes fabricated on top of the bulk substrate material of the cell, after etching off of the solar-cell structure, did not show the presence of the traps. The results suggest that defects, influencing the performance of solar cells, were formed in/near to the pn-junctions during their fabrication. The possible origin of the defects will be discussed.

© 2013 AIP Publishing LLC. [<http://dx.doi.org/10.1063/1.4807142>]

The ongoing struggle for higher efficiencies of photovoltaic-cells (solar cells) and for the reduction of production costs requires sensitive methods for detection and identification of defects, which are responsible for degrading the charge carrier lifetime. Carrier-lifetime sensitive measurement methods, i.e., photo- and electro-luminescence, microwave photoconductive decay ( $\mu$ -PCD), etc., can detect locations with degraded lifetime, but in most cases, they are unable to directly identify the defect(s) responsible for the degradation. Up to now, only bulk material of the cells was investigated<sup>1</sup> using deep level transient spectroscopy (DLTS) capable of defect identification. After removal of the solar cell structure, a Schottky diode was fabricated on the surface of the bulk material and carrier traps present in the depletion region of the diode were analyzed. Two drawbacks of the method are obvious. First, defects present in the pn-junction of the solar cell but absent in the wafer bulk escape detection. Second, preparation of the Schottky-diode includes polishing/etching procedures, which introduce hydrogen in the near surface volume of the material.<sup>2</sup> Hydrogen atoms may substantially alter the electrical activity of the defects present in the subsurface volume of the sample<sup>3</sup> and/or even introduce hydrogen-related defects there.<sup>4,5</sup> Therefore, it would be advantageous to perform DLTS measurements directly on the pn-junction of solar cells, with preserved structure and properties.

DLTS analyses of local pn-junctions of a solar cell were reported recently for Crystal-Silicon on Glass (CSG) samples.<sup>6</sup> In that work, the pn-junctions were separated from the surrounding cell material by laser-patterning. Such procedure comprises mostly uncontrollable heating of the material by the laser beam, possibly altering the defect content inside the Si layer.

In the present work, we used chemically resistant varnish to fabricate mesa-diodes on a fully processed solar cell wafer. Samples with sizes of  $5 \times 10 \text{ mm}^2$  were cut-out from the wafer retaining full electrical and optical structure of the solar cell, i.e., top Ag bus lines, anti-reflection layer, pn-junction, and sintered back Al contact. The areas of future mesa-diodes ( $\sim 1 \text{ mm}^2$ ) on the top of the sample and the

back-side Al Ohmic contact were covered with varnish and dried. Etching of the samples was performed in  $\text{HF} + \text{HNO}_3$  (1:5) solution, which dissolved the cell structure at the non-protected surface of the sample to the depth of  $\sim 50 \mu\text{m}$ . The varnish from the etched sample was removed by a solvent leaving behind mesa-diodes on the top of the sample and an Al Ohmic contact on its back. All fabrication operations were performed at room temperature. Areas of the fabricated mesa-diodes were estimated from their images. Each mesa-diode contained a part of the top Ag bus for contacting to the  $n^+$  volume of the  $n^+p$ -junction, while the p-type volume was contacted by the back Ohmic contact. To compare the traps in pn-junctions to those in the bulk material, the whole solar cell structure, except the back-side Al contact, was removed from the adjacent to the mesa-diode locations by etching to a  $50 \mu\text{m}$  depth. Aluminum dots with an area of  $1 \text{ mm}^2$  were deposited on the etched surface for Schottky contacts.

The samples for the DLTS measurements originated from solar cells, which were fabricated in a standard PV-process<sup>7,8</sup> using  $150 \mu\text{m}$  thick and  $156 \times 156 \text{ mm}^2$  squared Si wafers (B doped to  $\sim 3 \times 10^{15} \text{ cm}^{-3}$  level) cut-out from the mid and tail parts of the Cz-Si crystal specially grown using mixed feedstock Si material. Analyses of impurities content using Inductively Coupled Plasma Mass Spectrometry (ICP-MS) method revealed iron at the levels  $4 \times 10^{13} \text{ cm}^{-3}$  for the mid and  $1 \times 10^{14} \text{ cm}^{-3}$  for the tail parts of the crystal.<sup>9</sup> The solar cells were fabricated using consequent steps of KOH saw damage removal without texturization, RCA cleaning, P deposition coating, P diffusion, phosphorus silicate glass (PSG) removal and cleaning, deposition of antireflection coating ( $\text{Si}_3\text{N}_4$ ), Ag and Al contact deposition, and sintering of the contacts.

DLTS measurements were performed by means of a standard lock-in system working at the capacitance testing frequency of 1 MHz. Principles of the method and the system were previously described.<sup>10</sup> Cooling of a sample was done by immersion in a dewar with liquid He and a temperature controller maintained necessary temperature in the range of 35–300 K. Determination of exact parameters of the detected traps and depth profiling of their density were performed

using a Laplace DLTS (LDLTS) system,<sup>11</sup> equipped with a closed cycle He cryostat.

DLTS spectra detected for Schottky- and mesa-diodes located near the center of the solar cells, fabricated from the middle and the tail locations of the Cz-Si crystal are presented in Fig. 1. The spectra were measured under similar experimental conditions and the level of noise indicated the quality of the diodes in each case. Similar measurements were performed for several locations inside each cell along its diagonal. Besides the TM1 peak, visible in spectra 2 and 4 of Fig. 1, several other traps were detected. Namely, **FeB traps** (with energy level for the trap located at  $E_t = E_V + 0.08 \text{ eV}$ ) were detected in the Schottky diodes within  $\sim 5 \text{ mm}$  from the wafer edge. In the mesa-diodes, a deep trap for minority carriers ( $E_t = E_C - 0.39 \text{ eV}$ ) was detected for several randomly situated locations. In the mesa- and Schottky-diodes, a deep trap for majority carriers TM2 (see Fig. 1, spectra 3 and 4) with energy level position of  $E_t = E_V + 0.42 \text{ eV}$  and capture cross-section  $\sigma = 5 \times 10^{-18} \text{ cm}^2$  was detected near to the wafer edge and for the center locations of the wafers. However, only the TM1 peak was detected for almost all measured mesa-diodes and this peak was below the detection limit for the Schottky-diodes. The average amplitude of the TM1 peak was  $\sim 1.5$  times larger for the solar cells fabricated from the crystal tail than that for the cells fabricated from the mid position of the crystal. In the present letter, we will mainly discuss data related to the TM1 peak. Detailed results concerning the other traps will be presented elsewhere.

Precise parameters of the TM1 peak were determined from LDLTS measurements. Two traps, clearly seen in a high resolution spectrum in the inset of Fig. 2, with close parameters (TM1.1:  $E_t = E_V + 0.37 \text{ eV}$ ,  $\sigma = 3.1 \times 10^{-16} \text{ cm}^2$  and TM1.2:  $E_t = E_V + 0.42 \text{ eV}$ ,  $\sigma = 1 \times 10^{-15} \text{ cm}^2$ ) are responsible for the TM1 peak. Profiling of the trap density performed at 205 K using LDLTS under constant reverse bias conditions and a pair of coupled pulse voltages<sup>11</sup> showed a steep decrease in the trap densities with distance from the

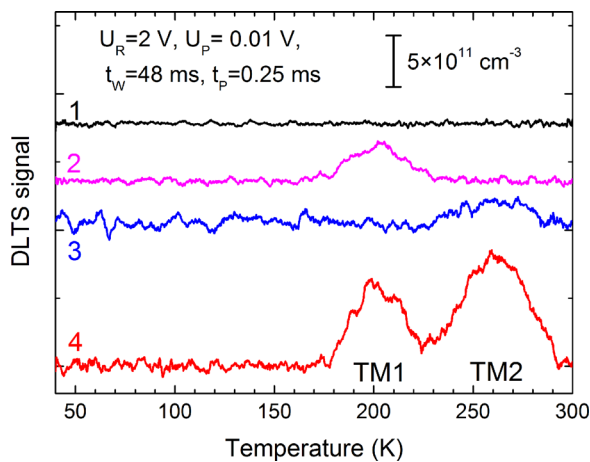


FIG. 1. DLTS spectra detected in Schottky-diodes (spectra 1 and 3) and mesa pn-junctions (spectra 2 and 4) fabricated from the solar cells using wafers from middle (1, 2) and tail (3, 4) parts of the Cz-Si crystal. The scale for trap density is indicated in the figure. Spectra are shifted vertically for convenience. The parameters of DLTS measurements are presented in the figure, where  $U_R$  is reverse bias,  $U_P$  is pulse bias,  $t_W$  is sampling time, and  $t_P$  is pulse duration.

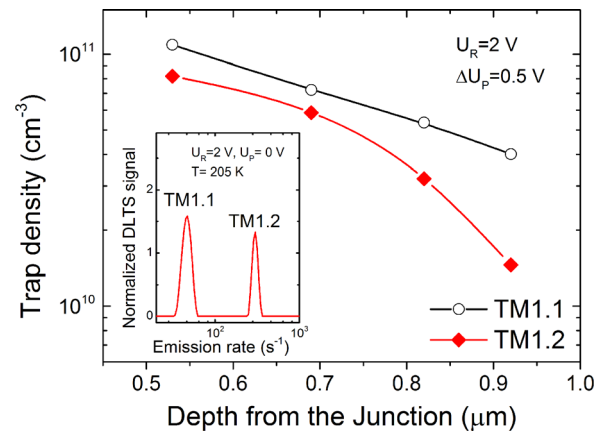


FIG. 2. Dependence of the TM1.1 and TM1.2 trap density on depth from the pn-junction of the solar cell. The inset presents LDLTS emission rate spectrum from the mesa-diode. Measurement parameters and curve attributions are indicated in the figure.

pn-junction (see Fig. 2). The absence of the TM1 signal for the Schottky-diodes located at neighbor to mesa-diodes positions but  $\sim 50 \mu\text{m}$  below the pn-junction level supports the steep profile for the trap density. The emission rates of the traps did not vary with the applied bias, suggesting that the traps are neutral before thermal excitation.<sup>12</sup> Absence of the dependence of the signal on the pulse length starting from  $t_P = 100 \mu\text{s}$  suggested that the DLTS signal originated from point-like traps.<sup>13</sup>

From the large variety of the defect-related traps reported for silicon, one should expect preferable formation of iron-related traps for the present sample, since iron (Fe) was the main contaminant in the feedstock. There are reports of at least several Fe-related traps with parameters similar to those of TM1.1 and TM1.2 in the literature (see, e.g., Refs. 14–18, and references therein). As seen from the Arrhenius plot in Fig. 3, the parameters of TM1.2 very well match to those reported for interstitial Fe-atom in Si.<sup>14–18</sup> Recently, a donor state of iron-vacancy pair, FeV with the energy level position at  $E_V + 0.35 \text{ eV}$  was predicted from theoretical calculations.<sup>19</sup> Moreover, a trap with the parameters close to those for TM1.1, detected in Fe contaminated samples after gettering procedure was ascribed to FeV.<sup>16</sup>

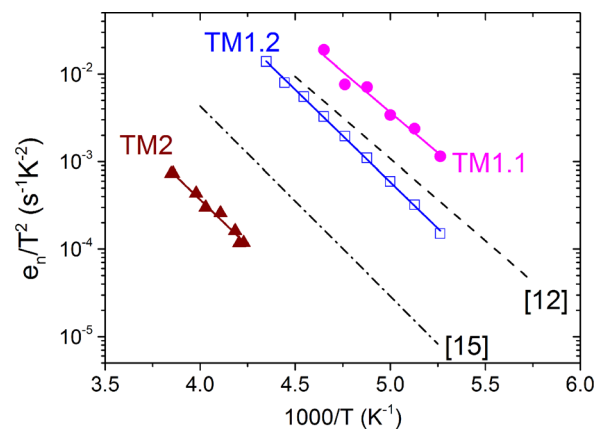


FIG. 3. Arrhenius plots for the TM1.1, TM1.2, and TM2 traps. Symbols present experimental results and fitted lines give estimates for the trap parameters indicated in the text. Dashed and dotted-dashed lines present previously published data for  $\text{Fe}_i$  (see Refs. 12 and 15).

The formation mechanism of Fe and vacancy containing defects in the vicinity of the pn-junction could be related with an inflow of vacancies from the region of P diffusion<sup>20</sup> and an outflow of Fe atoms from the wafer bulk due to the gettering process.<sup>16,21</sup> After finish of the P diffusion process, residual Fe and vacancy containing species may remain in the vicinity of the junction. Since the volume near the junction is subjected to an internal electric field of the diode, pairing of Fe atoms with boron, occurring in p-type Si due to the Coulomb interaction,<sup>14</sup> is not probable, thus, Fe atoms either remain at interstitial positions or form complexes with vacancies. A complex containing Fe, phosphorus and, possibly vacancy FeP (FeVP) was reported previously from ESR investigations.<sup>22</sup> Since all the components of such complex are present during gettering process near to the pn-junction its formation also cannot be excluded.<sup>21</sup> Therefore, a possible origin of TM1.1 trap, besides FeV pairs, can be also FeP complexes.

The difference in the TM1.1 and TM1.2 trap densities between the wafers from the mid and the tail positions in the crystal supports the proposed explanation, since the tail contained larger Fe concentrations. The detected traps may result from an incomplete Fe gettering process during phosphorus diffusion and deteriorate the solar cell performance. The obtained results suggest that the solar cell fabrication process should be tailored according to the feedstock used in the crystal growth process. On the other hand, measurements of carrier traps in the fabricated solar cells using DLTS could be applied for the control of the fabrication process suitability.

In summary, DLTS measurements on mesa-structures containing pn-junctions of solar cells revealed carrier traps which were not detected in the bulk material of the cell. These traps will definitely degrade solar cell efficiency; therefore, their detection and identification will allow further improvements for the cell fabrication process. The applied method of mesa-diode fabrication fully preserves the initial structure and the defect content of the cell, thus, allowing characterization of the pn-junction volume at the desired location inside the cell area. Moreover, differently from Schottky-diodes, traps for majority and for minority carriers could be detected and characterized for pn-junctions. Our experiments revealed the presence of presumably Fe-related traps in the volume of the pn-junction of the cell which could result from unaccomplished Fe-gettering process during

P-diffusion. A similar technique of mesa-diode characterization by DLTS, with minor modifications, could be applied for the analyses of pn-junctions at various solar cell fabrication stages after the P diffusion process.

The work was supported by the German Ministry for Education and Research under Contract No. 03SF0398K ( $\chi\mu$ -Material) in the framework of the Excellence Cluster Solar Valley Central Germany.

- <sup>1</sup>A. A. Istratov, H. Hieslmair, O. F. Vyvenko, E. R. Weber, and R. Schindler, *Sol. Energy Mater. Sol. Cells* **72**, 441 (2002).
- <sup>2</sup>C. H. Seager, R. A. Anderson, and J. K. G. Panotz, *J. Mater. Res.* **2**, 96 (1987).
- <sup>3</sup>J.-U. Sachse, E. Ö. Sveinbjörnsson, N. Yarykin, and J. Weber, *Mater. Sci. Eng., B* **58**, 134 (1999).
- <sup>4</sup>M. Yoneta, Y. Kamiura, and F. Hashimoto, *J. Appl. Phys.* **70**, 1295 (1991).
- <sup>5</sup>A. Endrös, W. Krühler, and J. Grabmeier, *Mater. Sci. Eng., B* **4**, 35 (1989).
- <sup>6</sup>T. Mchedlidze and M. Kittler, *J. Appl. Phys.* **111**, 053706 (2012).
- <sup>7</sup>J. Szlufcik, F. Duerinckx, E. van Kerschaver, R. Einhaus, A. Ziebakowski, E. Vazsonyi, K. D. Clercq, J. Horzel, L. Frisson, J. Nijs, and R. Mertens, in *Proceedings of the 14th European Photovoltaic Solar Energy Conference, WIP-Munich, Germany* (1997), p. 380.
- <sup>8</sup>T. Saga, *NPG Asia Mater.* **2**, 96 (2010).
- <sup>9</sup>K. Lauer, C. Möller, K. Neckermann, M. Herms, T. Mchedlidze, J. Weber, and S. Meyer, "Impact of a p-type solar cell process on the electrical quality of Czochralski silicon," *Energy Procedia* (in press).
- <sup>10</sup>G. L. Miller, D. V. Lang, and L. C. Kimmerling, *Annu. Rev. Mater. Sci.* **7**, 377 (1977).
- <sup>11</sup>L. Dobaczewski, A. R. Peaker, and K. Bonde Nielsen, *J. Appl. Phys.* **96**, 4689 (2004).
- <sup>12</sup>S. D. Ganichev, E. Ziemann, W. Prettl, I. N. Yassievich, A. A. Istratov, and E. R. Weber, *Phys. Rev. B* **61**, 10361 (2000).
- <sup>13</sup>W. Schröter, J. Kronewitz, U. Gnauert, F. Riedel, and M. Seibt, *Phys. Rev. B* **52**, 13726 (1995).
- <sup>14</sup>A. A. Istratov, H. Hieslmair, and E. R. Weber, *Appl. Phys. A* **69**, 13 (1999).
- <sup>15</sup>P. Kaminski, R. Kozłowski, A. Jelenski, T. Mchedlidze, and M. Suezawa, *Jpn. J. Appl. Phys., Part 1* **42**, 5415 (2003).
- <sup>16</sup>D. Abdelbarey, V. Kveder, W. Schröter, and M. Seibt, *J. Appl. Phys.* **108**, 043519 (2010).
- <sup>17</sup>K. Wünnel and P. Wagner, *Appl. Phys. A* **27**, 207 (1982).
- <sup>18</sup>T. Sadoh, K. Tsukamoto, A. Baba, D. Bai, A. Kenjo, and T. Tsurushima, *J. Appl. Phys.* **82**, 3828 (1997).
- <sup>19</sup>S. K. Estreicher, M. Sanati, and N. Gonzalez Szwacki, *Phys. Rev. B* **77**, 125214 (2008).
- <sup>20</sup>A. Bentzen, A. Holt, J. S. Christensen, and B. G. Svensson, *J. Appl. Phys.* **99**, 064502 (2006).
- <sup>21</sup>M. Syre, S. Karazhanov, B. R. Olaisen, A. Holt, and B. G. Svensson, *J. Appl. Phys.* **110**, 024912 (2011).
- <sup>22</sup>T. Mchedlidze and M. Suezawa, *J. Phys.: Condens. Matter* **16**, L79 (2004).